The Canadian Mineralogist
Vol. 34, pp. 411-421 (1996)

DIOPSIDE PHENOCRYSTS FROM NEPHELINITE LAVAS, NAPAK VOLCANO, EASTERN UGANDA: EVIDENCE FOR MAGMA MIXING

ANTONIO SIMONETTI[1]

Ottawa-Carleton Geoscience Centre, Department of Earth Sciences, Carleton University, 1125 Colonel By Drive, Ottawa, Ontario K1S 5B6

MARK SHORE

Ottawa-Carleton Geoscience Centre, Department of Geology, University of Ottawa, Ottawa, Ontario K1N 6N5

KEITH BELL

Ottawa-Carleton Geoscience Centre, Department of Earth Sciences, Carleton University, 1125 Colonel By Drive, Ottawa, Ontario K1S 5B6

Abstract

Samples of olivine nephelinite from Napak volcano, eastern Uganda, contain two populations of clinopyroxene phenocrysts, one chromian and the other titanium-bearing aluminian diopside. The chromian diopside crystals are among the most magnesian to occur in nephelinite. The diopside phenocrysts show normal, reverse and oscillatory zoning, and some have an embayed texture suggestive of resorption. Disequilibrium in Nd, Pb, and Sr isotopic ratios for both populations of clinopyroxene and their host rocks is interpreted in terms of crystallization in an open system. Populations of chromian and Ti-bearing aluminian diopside from the same lavas have distinct isotopic ratios, indicative of derivation and crystallization from different melts. We attribute the zoning, textural features, and bimodality of the Napak diopsides to the mixing of at least two nephelinitic magmas at a shallow crustal level.

Keywords: diopside, bimodality, magma mixing, nephelinite, Napak, Uganda.

Sommaire

La néphélinite à olivine du volcan Napak, en Ouganda oriental, contient deux populations de phénocristaux de clinopyroxène, le premier un diopside chromifère, et l'autre, un diopside titanifère alumineux. Les cristaux de diopside chromifère sont parmi les plus magnésiens que l'on puisse trouver dans une néphélinite. Les phénocristaux démontrent des séquences de zonation normale, renversée, et oscillatoire, et dans certains cas, une morphologie améboïde qui pourrait indiquer une résorption. Les rapports des isotopes de Nd, Pb et Sr des deux populations de clinopyroxène et de leurs roches hôtes témoignent d'un déséquilibre; nous l'interprétons en termes de cristallisation en système ouvert. Les deux sortes de diopside provenant des mêmes échantillons de lave possèdent des rapports isotopiques distincts, indication d'une dérivation par cristallisation de magmas distincts. Nous attribuons la zonation, la texture, et la bimodalité des diopsides à Napak au mélange d'au moins deux magmas néphéliniques à faible profondeur dans la croûte.

(Traduit par la Rédaction)

Mots-clés: diopside, bimodalité, mélange de magmas, néphélinite, Napak, Ouganda.

Introduction

Regions of continental rifting are commonly associated with alkaline igneous activity. One such example is the East African Rift Valley System. In addition to the large outpourings of alkali basalt, phonolite and trachyte that occur in the northeast part of the rift, alkaline igneous activity may also take the form of discrete eruptive centers associated with carbonatitic and nephelinitic magmatism. One of these, Napak in Uganda, is the eroded remnant of a carbonatite–nephelinite volcano (Latitude: 2°0′ to 2°15′ N; Longitude: 34°10′ to 34°25′E).

[1] Present address: Max-Planck-Institut für Chemie, Abteilung Geochemie, Postfach 3060, D-55020 Mainz, Germany.

Derivation of nephelinitic magma is consistent with small degrees of partial melting of a carbonated peridotite (Brey & Green 1977, Brey 1978, Olafsson & Eggler 1983, Wallace & Green 1988) or amphibole peridotite (Olafsson & Eggler 1983, Eggler 1989) at pressures of 20 to 25 kbar. Nephelinitic and carbonatitic melts are typically found together, and are thus considered cogenetic, forming by either liquid immiscibility from a common carbonated olivine nephelinitic parent magma at crustal pressures (Freestone & Hamilton 1980, Kjarsgaard & Peterson 1991) in alkali- or Ca-rich systems (Koster van Groos & Wyllie 1966, 1968, 1973, Wendlandt & Harrison 1979, Kjarsgaard & Hamilton 1988, 1989a, b, c), or by fractional crystallization (Le Bas 1989).

Fractionation of nephelinitic magmas involves major phenocryst phases such as olivine, clinopyroxene, nepheline, and Fe–Ti oxides (Peterson 1989b); of these, clinopyroxene is probably the most useful in monitoring the evolution of nephelinitic magma. Clinopyroxene remains on the liquidus over a wide range of melt temperature (*e.g.*, 1100° to 1600°C: Bultitude & Green 1971, Thompson 1974) and melt composition, incorporates measurable amounts of minor and trace elements, and is relatively slow to re-equilibrate through diffusion (*e.g.*, Shimizu 1990).

Previous studies of clinopyroxene phenocrysts from nephelinite (*e.g.*, Le Bas 1987, Donaldson *et al.* 1987), basanite (*e.g.*, Duda & Schmincke 1985, Dobosi & Fodor 1992), and alkali basalt (*e.g.*, Wass 1979) commonly show crystals that are highly zoned and partially resorbed, suggesting a complex history of crystallization. Complexly zoned phenocrysts of clinopyroxene have been documented from the peralkaline nephelinite lavas from the only active carbonatite–nephelinite volcano, Oldoinyo Lengai (Tanzania), as well as nearby Shombole volcano (both in Peterson 1989a). In addition, lavas from a number of alkaline volcanic centers (*e.g.*, Wass 1979, Barton & van Bergen 1981, Duda & Schmincke 1985, Dobosi & Fodor 1992) contain different populations of clinopyroxene with distinct chemical compositions.

TABLE 1. AVERAGE COMPOSITIONS OF DIOPSIDE PHENOCRYSTS FROM NAPAK

Sample	TL 874	TL 971	TL 973	NP 100	NP 100	NP 101	NP 112	NP 112
Type	Ti-Al	Ti-Al	Ti-Al	Ti-Al	Cr-Mg	Ti-Al	Ti-Al	Cr-Mg
# anal.	16	11	18	15	15	40	47	39
SiO_2	50.3 (2.05)	50.9 (1.23)	50.3 (0.79)	51.5 (1.04)	53.6 (0.45)	50.6 (0.82)	50.3 (0.99)	53.2 (0.73)
TiO_2	1.3 (0.63)	1.0 (0.30)	1.2 (0.18)	0.9 (0.20)	0.4 (0.05)	1.0 (0.19)	1.3 (0.24)	0.5 (0.17)
Al_2O_3	3.6 (1.55)	2.5 (1.09)	3.3 (0.45)	3.0 (0.64)	1.1 (0.17)	3.3 (0.52)	3.4 (0.93)	1.3 (0.33)
Cr_2O_3	0.2 (0.16)	0.5 (0.56)	0.1 (0.06)	0.1 (0.09)	0.6 (0.26)	0.2 (0.16)	0.1 (0.13)	0.7 (0.39)
FeO	6.6 (1.63)	5.4 (0.96)	6.3 (0.55)	5.4 (0.67)	3.2 (0.24)	6.3 (0.83)	6.7 (0.62)	3.6 (0.68)
MgO	14.1 (1.54)	14.8 (0.87)	14.3 (0.64)	15.2 (0.61)	17.4 (0.31)	14.7 (0.68)	14.2 (0.51)	16.7 (0.57)
MnO	0.0 (0.08)	0.0 (0.04)	0.0 (0.03)	0.0 (0.03)	0.0 (0.03)	0.0 (0.04)	0 0 (0.03)	0.0 (0.04)
CaO	22.4 (0.50)	23.4 (0.03)	22.7 (0.30)	22.3 (0.26)	22.4 (0.22)	21.8 (0.19)	22.8 (0.71)	22.8 (0.51)
Na_2O	0.6 (0.46)	0.4 (0.24)	0.3 (0.18)	0.9 (0.19)	0.7 (0.10)	0.7 (0.21)	0.6 (0.30)	0.5 (0.23)
Total	99.3	99.3	98.8	99.6	99.7	98.9	99.9	99.6
			Formula Proportions* Based On 4 cations and 6 Oxygen Atoms					
Si	1.869	1.890	1.882	1.892	1.948	1.881	1.861	1.948
Al^{IV}	0.131	0.110	0.118	0.108	0.050	0.119	0.139	0.052
Al^{VI}	0.027	0.001	0.029	0.021	0.000	0.027	0.013	0.005
Ti	0.037	0.029	0.035	0.026	0.011	0.030	0.037	0.014
Cr	0.007	0.016	0.005	0.005	0.017	0.007	0.006	0.022
Fe^{3+}	0.067	0.068	0.038	0.095	0.074	0.078	0.092	0.037
Fe^{2+}	0.139	0.100	0.159	0.075	0.025	0.118	0.118	0.075
Mg	0.783	0.821	0.800	0.835	0.944	0.815	0.783	0.915
Mn	0.002	0.001	0.001	0.001	0.001	0.001	0.001	0.001
Ca	0.894	0.929	0.909	0.877	0.873	0.868	0.905	0.893
Na	0.045	0.034	0.024	0.066	0.056	0.055	0.046	0.038
Sum	4.000	4.000	4.000	4.000	4.000	4.000	4.000	4.000
			Normalized End-Member Molar Proportions					
Wo	0.474	0.484	0.477	0.466	0.455	0.462	0.477	0.465
Fs	0.110	0.088	0.104	0.091	0.052	0.105	0.111	0.059
En	0.415	0.428	0.420	0.443	0.492	0.434	0.412	0.476
Mg #	0.78	0.83	0.80	0.83	0.91	0.81	0.79	0.89

*: Fe^{3+} content was calculated stoichiometrically (Droop 1987). Average wt% values are followed in brackets by one sigma standard deviation. Microprobe analyses were determined using a Cambridge Microscan 5 EDS system. Operating conditions were 20 kV accelerating potential and a beam current (absorbed) of 10 nA measured on an amphibole standard. Raw X-ray spectra were reduced by the EDDI program (Pringle 1989). Uncertainties: major oxides, 2% of the quoted value; minor oxides, <5 wt% (5%), < 1 wt% (10%). Compositions are expressed as molar end-members Wo (Ca cation proportions), Fs (Fe^{2+} + Fe^{3+} + Mn cation proportions), and En (Mg cation proportions).

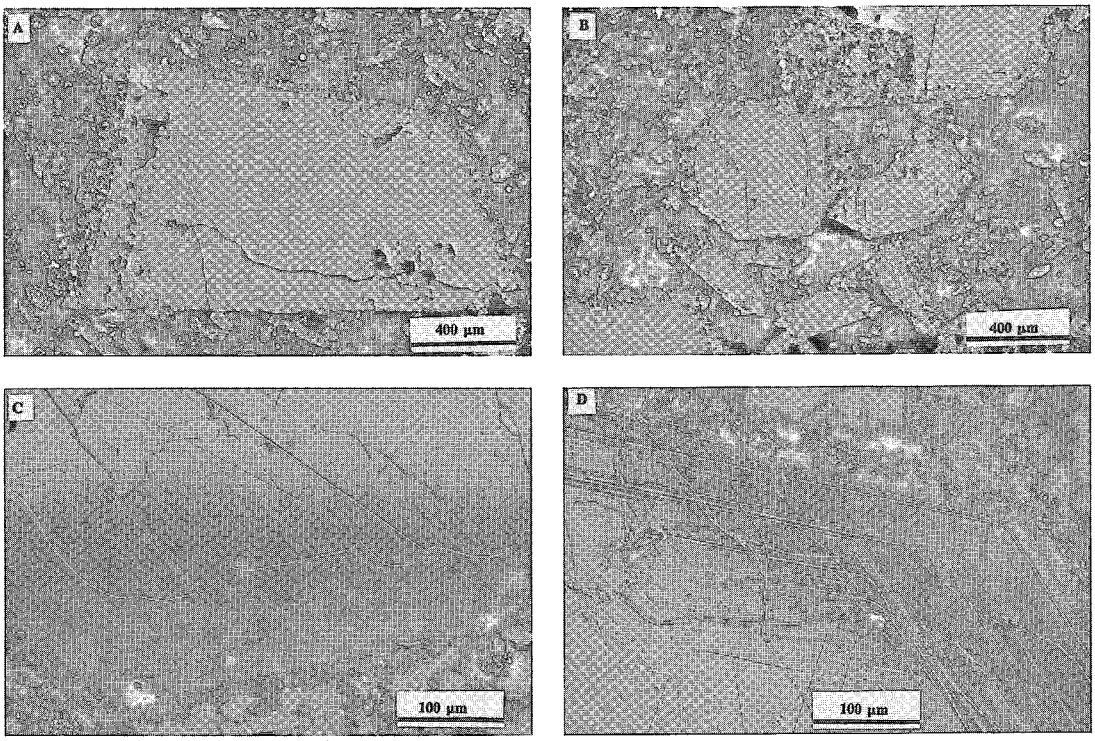

FIG. 1. Nomarski interference contrast (NIC) microphotographs of diopside phenocrysts from Napak nephelinite lavas. In minerals, subtle compositional variations can be detected with a spatial resolution on the order of 1 μm. For this study, polished sections were etched in a 1:1:1 mixture of concentrated hydrochloric, hydrofluoric, and citric acids. Nomarski interference microphotographs from samples NP 102 and NP 112 show: (A) typical diopside phenocryst, with an unzoned core, oscillatory zoned mantle of Ti-bearing aluminian diopside, and a "spongy" margin; (B) a group of diopside phenocrysts showing variations in zoning and extent of core resorption; (C) a diopside phenocryst showing at least two episodes of resorption (the core has rounded corners and cuspate re-entrants, mantled subsequently by oscillatory zoned layers); (D) irregular zoning associated with diopside core, subsequently overgrown by zoned outer layers.

Studies of nephelinite lavas from Napak, and of their populations of diopside phenocrysts (Simonetti & Bell 1993), reveal that the pyroxenes have Nd, Pb, and Sr isotopic compositions that are not in equilibrium with their host rocks, and are inconsistent with closed-system, equilibrium crystallization of a single parental magma. The difference in Nd, Pb and Sr isotopic ratios between the diopside phenocrysts and their corresponding host-rocks cannot be attributed to processes of magmatic differentiation, such as polybaric fractionation of crystals from one parental melt. Disequilibrium (Simonetti & Bell 1993) could be attributed to either the mixing of melts derived from an isotopically heterogeneous upper mantle, or assimilation of lower-crust granulite (Simonetti & Bell 1994). In addition, the consistent values of the Mg# [100*Mg/(Mg + Fe^{2+}), 61–80] of the Napak nephelinite lavas argue against closed-system differentiation of a single magma (Simonetti & Bell 1994).

Here, we present the results of more than 250 electron-microprobe analyses of diopside phenocrysts and titaniferous magnetite from six samples of nephelinite lava from Napak. We used these results to determine: (1) the crystallization history of the Napak lavas, and (2) the role of open-system behavior, *i.e.*, an evaluation of crustal contamination of a single parental magma *versus* magma mixing to explain the data from Napak.

GEOLOGY

Napak is considered unique among the many eastern Ugandan Tertiary nephelinite–carbonatite centers because both extrusive and intrusive rocks are exposed. A central carbonatite–ijolite plug is flanked by deeply dissected agglomerates, tuffs, and silica-undersaturated flows that overlie Precambrian basement, consisting of quartzofeldspathic gneiss and granulite. Pyroclastic

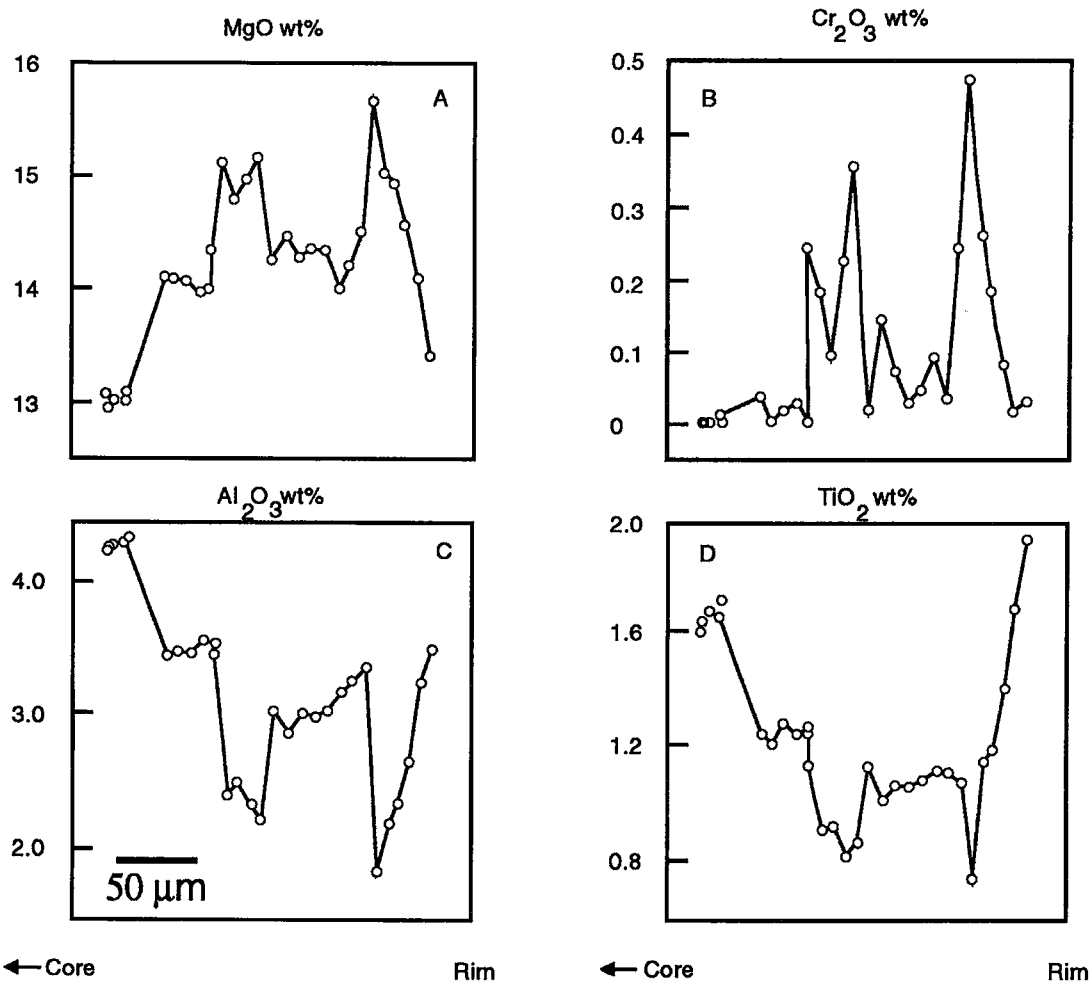

FIG. 2. Major-element variations (in wt% oxide) along a core-to-rim traverse across a phenocryst of Ti-bearing aluminian diopside (sample TL 973). (A) MgO, (B) Cr_2O_3, (C) Al_2O_3, and (D) TiO_2. Traverses were obtained using a CAMECA electron microprobe (Department of Earth and Planetary Sciences, McGill University). Run conditions were: spot size of 2 µm, accelerating potential of 15 kV and current (standardized on a variety of silicates and oxides) of 20 nA. Uncertainties for the MgO, Al_2O_3, and TiO_2 are ±2% of the quoted values above 1 wt%.

rocks form ~97% of the Napak exposures; the remainder consists of silica-undersaturated lavas, mostly nephelinitic in composition. About 1% by volume of the lavas consist of silica-saturated (quartz- and albite-normative) "andesitic" flows (King 1949).

The Napak suite of nephelinite samples has been divided into olivine-bearing, olivine-free, and melilite nephelinites (King 1949, Simonetti & Bell 1994). The olivine-bearing nephelinite contains phenocrysts of olivine, diopside, and titaniferous magnetite; only diopside and titaniferous magnetite occur in the olivine-free nephelinite. The groundmass of all three groups consists mainly of fine-grained clinopyroxene, nepheline and titaniferous magnetite. The olivine-bearing and olivine-free nephelinites have a high Mg# (61 to 80), a range considered characteristic of primary mantle-derived melts (Roeder & Emslie 1970).

RESULTS

Diopside phenocrysts

Compositions of diopside phenocrysts from Napak are given in Table 1. These range from highly magnesian chromian diopside to titanium-bearing aluminian diopside. Two of the samples, NP 100 and NP 112, contain at least two populations of clinopyroxene (light green chromian diopside, and dark

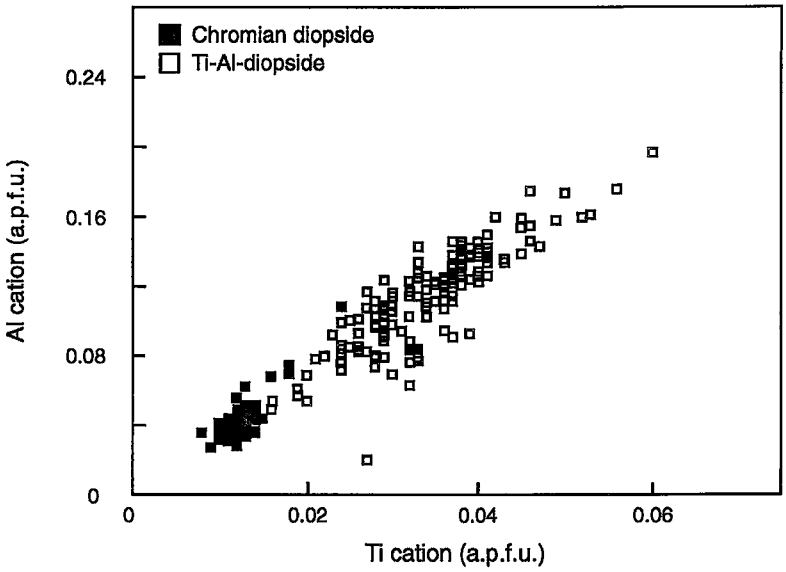

FIG. 3. Plot of Al *versus* Ti cation proportions for all Napak diopside phenocrysts, expressed in atoms per formula unit (apfu).

green titanium-bearing aluminian diopside) that form cores to the phenocrysts, with either a normally or a reversely zoned mantle.

Variations in major-element contents within individual, highly zoned diopside phenocrysts can span most of the compositional range of Napak diopside. Nomarski interference contrast (NIC) photomicrographs (Anderson 1983, Clark *et al.* 1986) of Napak diopside phenocrysts (Fig. 1) and electron-microprobe traverses (Fig. 2) reveal: (a) growth bands (normally or reversely zoned) of variable thickness, (b) fine-scale oscillatory zoning, (c) rounded corners for many of the euhedral crystals, (d) embayed faces, and partially dissolved or resorbed cores. A variety of representative patterns of zoning revealed by NIC microscopy are shown in Figure 1. The unzoned to weakly zoned cores, typically bounded by curved, cuspate, or irregular resorption-induced surfaces, may be attributed to slow growth and re-equilibration prior to partial resorption. The irregular, inclusion-rich margins are most likely due to post-eruptive growth (Figs. 1A, B, D).

The origin of fine-scale oscillatory zoning in silicate phases is unclear, but may reflect changes in the bulk composition of the melt, temperature, pressure and redox state (Pearce & Kolisnik 1990, Reeder *et al.* 1990, Shimizu 1990). Figure 2 shows the distribution of Mg, Cr, Ti, and Al in a reversely zoned phenocryst of titanium-bearing, aluminian diopside. The antithetic variation of Mg and Cr with Al and Ti is similar to elemental variations in oscillatory-zoned diopside phenocrysts from other alkaline volcanic rocks (*e.g.*, Thompson 1973, Shimizu 1990).

The two populations of pyroxene have the same Al:Ti ratio, with the chromian diopside spanning a narrower compositional range than the titanium-bearing aluminian diopside (Fig. 3). The Cr (up to 1.8 wt% Cr_2O_3) and Mg contents (in most cases >16 wt% MgO) of the chromian diopside suite at Napak are unusually high for diopside from nephelinite

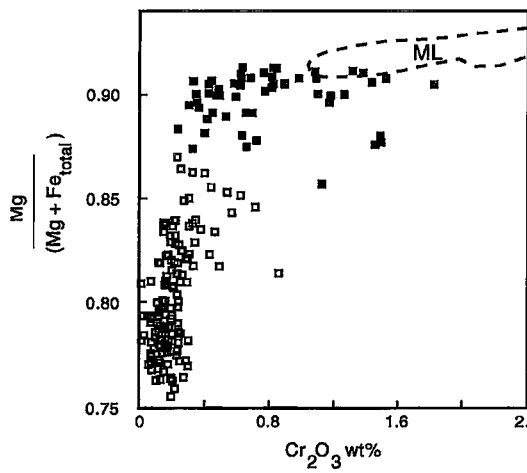

FIG. 4. Plot of $Mg/(Mg + Fe_{total})$ *versus* proportion of Cr_2O_3 (wt%) for Napak suite of clinopyroxene. Symbols as in Fig. 3. ML: field of clinopyroxene compositions from mantle lherzolite, characteristic of all chromian diopside xenocrysts [*e.g.*, Lashaine tuff cone, Tanzania, Cohen *et al.* (1984), Dawson (1987)].

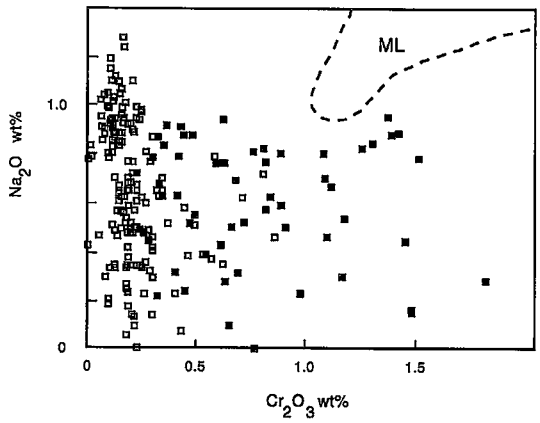

FIG. 5. Plot of proportion of Na_2O *versus* Cr_2O_3 (wt%) for Napak suite of diopside. Symbols as in Fig. 3. Mantle peridotite field, taken from Schulze (1987), encompasses compositions of clinopyroxene from lherzolite from Lashaine, Tanzania (Cohen *et al.* 1984, Dawson 1987).

(*e.g.*, Donaldson *et al.* 1987, Le Bas 1987, Peterson 1989a, Upton *et al.* 1992), but are similar to the levels noted in pyroxene of mantle origin. In Figures 4 and 5, we compare data from the Napak diopside suites with those from mantle xenoliths. Although some of the chromian diopside compositions from Napak have Cr contents similar to clinopyroxene from mantle lherzolite, their Al (Table 1), Mg# (Fig. 4) and Na contents (Fig. 5) are lower than the latter (*e.g.*, Cohen *et al.* 1984, Dawson 1987). Few of the chromian diopside compositions from Napak plot within the fields for mantle lherzolite clinopyroxene (Figs. 4, 5). Other evidence that argues against the diopside being upper mantle xenocrysts includes their commonly euhedral habit, lack of deformation, and lack of inclusions of, or intergrowths with, high-pressure phases. The presence of a Cr-rich mantle around a titanium-bearing aluminian diopside core in several phenocrysts from Napak (*e.g.*, TL973, Fig. 2) is evidence in favor of a magmatic origin for the chromian diopside.

Progressive crystallization of olivine and diopside from a single batch of magma should produce a smooth increase in the Al and decrease in the Mg contents of clinopyroxene, and not the abrupt change shown in Figure 6B. The relatively uniform Mg content of the suite of chromian diopside (see Fig. 6) is somewhat difficult to explain because it can occur with olivine of composition Fo_{88-78} (Simonetti & Bell 1994), and Pearce element-ratio regressions of compositional data from olivine nephelinite samples indicate cofractionation of olivine and diopside (relative proportions: olivine 15 ± 10%, diopside 85 ± 10%, mean Mg# ≈83). All of the nephelinite samples studied from Napak contain the same assemblage of phenocrysts (diopside + titaniferous magnetite ± olivine), and it therefore seems unlikely that the abrupt change in Al shown in Figure 6B can be attributed to a change in the proportions of the phenocryst phases. The trends shown in Figures 6A and 6B suggest that the chromian and the titanium-bearing aluminian diopsides were probably not the products of crystallization from the same batch of magma. The calculated effect of Rayleigh fractionation on Cr, Al, Mg, and Fe, assuming a K_D of 0.3 for Fe/Mg, does not account for the sharp inflection shown in Figure 6. Another possible explanation for the chemical variations shown in Figure 6 may be an olivine-out reaction with the liquid, mired at a peritectic point, to produce clinopyroxene (*e.g.*, Ne–Di–Qtz system: Schairer & Yoder 1960, Ne–Di–Sa system: Platt & Edgar 1972). Although both fractional crystallization and an olivine-out peritectic reaction may explain the chemical changes illustrated in Figure 6, they cannot produce reverse zoning or the isotopic disequilibria observed in the Napak lavas.

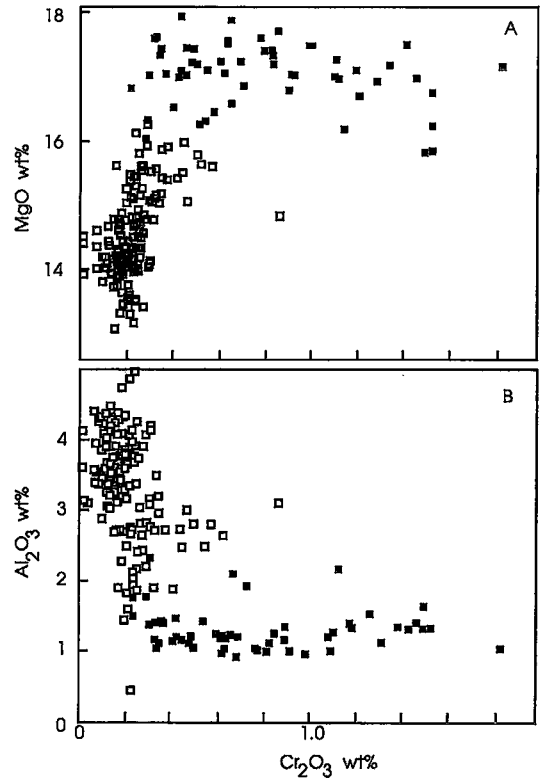

FIG. 6. Major-element variation diagrams for Napak suite of diopside. Symbols as in Fig. 3. (A) Proportion of MgO *versus* Cr_2O_3 (wt%); (B) proportion of Al_2O_3 *versus* Cr_2O_3 (wt%).

Titaniferous magnetite

Titaniferous magnetite in the Napak suite of nephelinite samples occurs as phenocrysts up to 5 mm across, as inclusions in diopside phenocrysts, and as small crystals in the groundmass. Representative compositions are given in Table 2. Most grains of titaniferous magnetite are unaltered, and only <5% of the phenocrysts show signs of incipient oxidation or exsolution. That the oxide inclusions are almost exclusively confined to the titanium-bearing, aluminian diopside phenocrysts suggests that conditions of crystallization, such as temperature (Santacroce *et al.* 1993) or oxygen fugacity, differed from those that existed during precipitation of the chromian diopside. Two inclusions of magnetite found in chromian diopside phenocrysts (sample NP 112) are very similar in composition to those found within the titanium-bearing aluminian diopside, although they do have higher Cr contents (Table 2). This similarity further supports a cognate origin for the chromian diopside suite.

Discussion

The most common clinopyroxene phenocrysts found in melanephelinite lavas consist of augite with low Al and Ti contents (Le Bas 1987), and these are usually zoned, with Al and Fe contents increasing outward, the direct result of magmatic differentiation. Pyroxene similar in composition to the suite of titanium-bearing aluminian diopside at Napak has been described from plutonic rocks, such as ijolite, associated with carbonatite complexes (*e.g.*, Fen: Mitchell 1980). However, recent Nd and Sr isotopic analyses of ijolite, the presumed plutonic equivalents of nephelinite, associated with two alkaline complexes (Illvara, Finland: Kramm 1994; Napak, Uganda: Simonetti & Bell 1994) indicate that the evolution of the ijolite was quite different to that of the associated nephelinite. Isotopic data from both studies suggest the involvement of crust in the formation of the ijolite; because of this, any comparison of pyroxene compositions from lavas and plutonic rocks is best avoided.

Aluminum-poor and Cr-rich diopside phenocrysts

TABLE 2. AVERAGE COMPOSITION OF Fe-Ti OXIDE, NEPHELINITE LAVAS, NAPAK

#	NP 100	NP 100	NP 102	NP 102	NP 102	NP 112	NP 112	NP 112	TL 973	TL 973	TL 973
Type	I	G	I	P	G	I	I*	G	I	P	G
# anal.	3	2	5	3	2	9	2	1	2	5	3
wt%											
SiO_2	0.18	0.27	0.26	0.22	0.40	0.22	0.29	0.00	0.12	0.20	0.22
Al_2O_3	3.88	0.32	2.61	2.10	0.66	3.37	3.11	1.32	4.26	3.18	0.48
TiO_2	12.05	17.29	14.37	16.25	18.10	12.73	11.94	15.97	11.69	13.73	17.81
Cr_2O_3	0	0.14	0.09	0	0	0.17	2.05	0.21	0	0.27	0.64
V_2O_3	0.10	0.40	0.30	0.33	0.22	0.30	0.26	0.20	0.18	0.11	0.31
FeO	72.20	74.06	72.33	72.19	71.74	72.24	70.64	73.68	71.65	71.84	71.31
MnO	0.29	0.85	0.74	0.89	0.94	0.41	0.38	0.63	0.35	0.65	0.80
MgO	4.52	1.10	2.52	1.30	0.34	4.38	4.17	1.80	5.16	3.70	3.03
CaO	0.10	0.08	0.10	0.08	0.26	0.25	0.44	0.00	0.1	0.09	0.19
Total	93.31	94.48	93.29	93.36	92.64	94.05	93.27	93.82	93.49	93.8	94.79
Formula Proportions** Based On 3 cations and 4 Oxygen Atoms											
Si	0.006	0.008	0.010	0.009	0.009	0.008	0.011	0.008	0.004	0.008	0.008
Al	0.169	0.014	0.116	0.094	0.031	0.146	0.137	0.059	0.183	0.139	0.021
Ti	0.334	0.498	0.408	0.469	0.535	0.352	0.335	0.456	0.321	0.384	0.502
Cr	0	0.004	0.003	0	0	0.005	0.060	0.006	0	0.008	0.019
V	0.003	0.012	0.009	0.010	0.007	0.009	0.008	0.006	0.005	0.003	0.009
Fe^{3+}	1.147	0.950	1.036	1.372	0.847	1.122	1.182	1.031	1.160	1.067	0.929
Fe^{2+}	1.079	1.421	1.249	0.940	1.511	1.097	1.011	1.310	1.030	1.162	1.309
Mn	0.009	0.028	0.024	0.029	0.031	0.013	0.012	0.020	0.011	0.020	0.026
Mg	0.248	0.062	0.142	0.073	0.019	0.240	0.232	0.102	0.281	0.205	0.170
Ca	0.004	0.003	0.010	0.003	0.011	0.010	0.018	0	0.004	0.004	0.008
Normalized End-members Mole Proportions											
Ulvosp	0.37	0.51	0.44	0.50	0.56	0.39	0.36	0.36	0.42	0.52	0.47
Mag.	0.63	0.49	0.56	0.50	0.44	0.61	0.64	0.64	0.58	0.48	0.53

*: Analyses obtained from chromian diopside phenocryst host.

**: Fe^{3+} content was calculated stoichiometrically (Droop 1987). Types: I = inclusions in diopside phenocrysts; P= phenocrysts; G = groundmass crystals. Oxide analyses were obtained on a JEOL 6400 digital SEM coupled to a LINK EXL L24 x-ray analyzer using the energy dispersive system (EDS). Data was collected using a 30 square mm detector and 133 electron volt resolution @ MnK-alpha. Operating conditions were: 20 kV accelerating potential, 40^0 take off angle, 0.8 nA absorbed current, and count time of 120 seconds. Natural sample and synthetic oxide standard analyses were reduced using the LINK ZAF 4/FLS computer program. Relative uncertainties: major oxides (> 5wt%), 2% of quoted value; minor elements 5.0 wt% (2%) - 0.5 wt% (10%). Minimum detection limit is ~ 0.1 wt%.

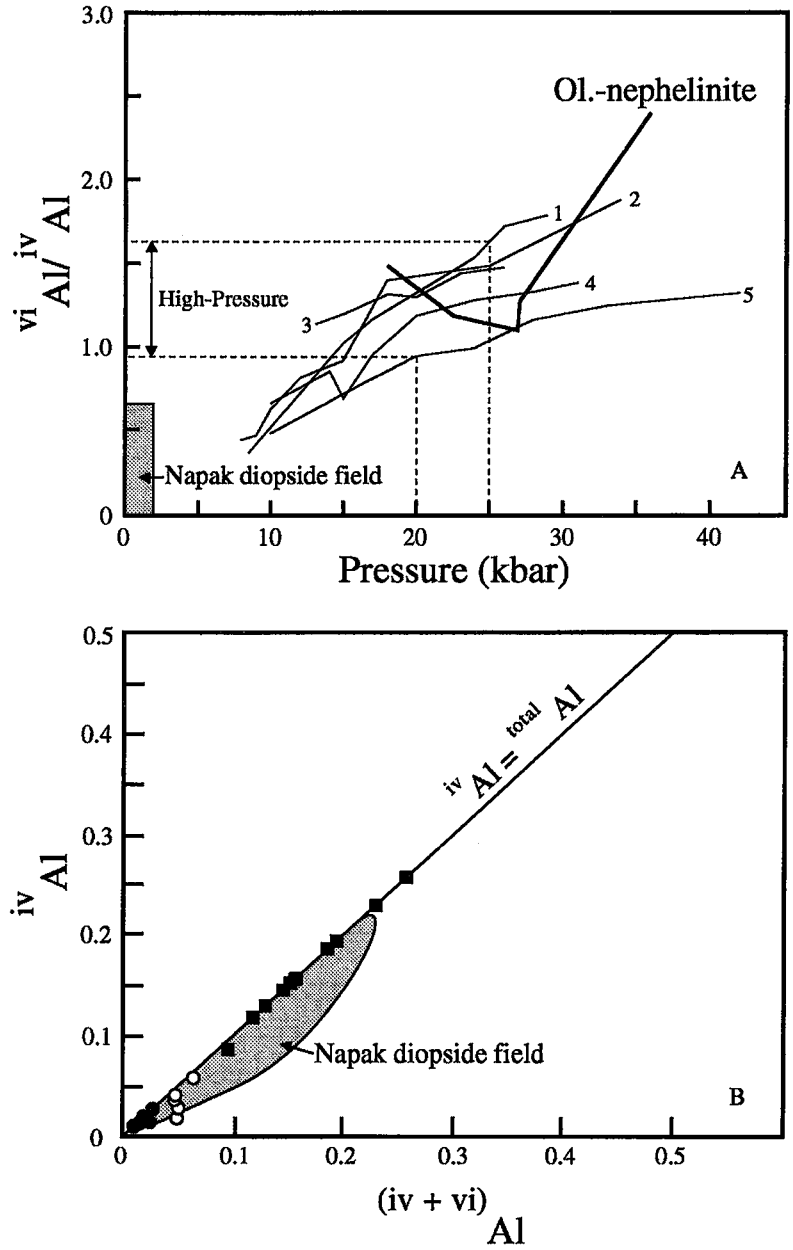

FIG. 7. (A) Plot showing variation of $^{VI}Al/^{IV}Al$ with pressure of crystallization for liquidus calcic clinopyroxene (Thompson 1974): 1 tholeiitic andesite, 2 olivine tholeiite, 3 transitional basalt, 4 olivine-rich, alkaline basalt, 5 augite-bearing leucitite. Results from olivine nephelinite are from Bultitude & Green (1971). (B) Diagram of ^{IV}Al *versus* $^{(total)}Al$ for clinopyroxene of low-pressure origin: Solid squares: low-pressure clinopyroxene from Wass (1979). Note that the pyroxene compositions of Wass (1979) have been stoichiometrically recalculated (Droop 1987). Open circles: pyroxene from Shombole nephelinite (Peterson 1989a), solid circles: pyroxene from Oldoinyo Lengai nephelinite (Peterson 1989a).

similar to those from Napak have been found in other nephelinite lavas, but are uncommon. Depending on their mode of occurrence, such as disaggregated crystals or pyroxenite blocks, they have either been considered mantle xenocrysts or deeply formed cumulates (Le Bas 1987). Compared to the chromian diopside at Napak, clinopyroxene microphenocrysts from dykes of primitive (Mg# ≈ 73) olivine melanephelinite from the Orkney Islands (Scotland) have much lower Mg (10.39 to 11.64 wt% MgO) and SiO_2 (39.80 to 44.60 wt%) contents, similar Na (0.35 to 0.76 wt% Na_2O), Ca (22.27 to 23.85 wt% CaO) and Fe (6.39 to 7.57 wt% FeO) contents, but much higher Al (8.91 to 11.68 wt% Al_2O_3; Upton *et al.* 1992). The high Mg and Cr contents of the Napak chromian diopside may indicate crystallization from an unusually primitive nephelinitic magma; as an alternative, high $CO_2/(CO_2 + H_2O)$ may have acted to increase melt polymerization and enlarge the stability field of diopside at the expense of olivine ± chromian spinel

(B.A. Kjarsgaard, unpubl. data, 1993).

The depth of crystallization of the chromian diopside suite at Napak can be evaluated by a comparison with clinopyroxene compositions (Mg# of 86 to 89) in the high-pressure experiments of Bultitude & Green (1971), who used olivine nephelinite as the starting material (Fig. 7A). These results show that liquidus or near-liquidus clinopyroxene from olivine nephelinite is Al-rich (>10 wt% Al_2O_3), with total Al and ^{VI}Al content increasing with pressure. The aluminum content of calcic clinopyroxene is determined by several factors that include: alkalinity, silica activity (basic alkaline rocks can have a significant extent of substitution of ^{IV}Al for Si), and pressure (increasing pressure favors incorporation of ^{VI}Al: Deer *et al.* 1992). Figure 7A shows the $^{VI}Al/^{IV}Al$ values of clinopyroxene formed in melts of various compositions, including olivine nephelinite, at pressures of between 20 to 25 kbar (the approximate depth of generation of nephelinitic melt) should range from 1.0 to 1.5 (Bultitude & Green 1971, Thompson 1974). In contrast, the compositions for the suite of diopside from Napak have $^{VI}Al/^{IV}Al$ values that are substantially different (0 to 0.65, Fig. 7A), and these are more typical of low-pressure (<10 kbar) igneous clinopyroxene (Aoki & Kushiro 1968, Aoki & Shiba 1973).

In calcic clinopyroxene, the $^{VI}Al/^{IV}Al$ value can be used as a crude empirical geobarometer (*e.g.*, Wass 1979, Meyer & Mitchell 1988). The distribution of Al between octahedral and tetrahedral sites ($^{VI}Al/^{IV}Al$) for the pyroxenes from Napak can be calculated from microprobe data and mineral stoichiometry. In Figure 7B, the Napak suite of diopside follows a trend similar to that defined by clinopyroxene of low-pressure origin (where $^{IV}Al \approx$ total Al), which further supports shallow-level crystallization. On the basis of the low $^{VI}Al/^{IV}Al$ values for the Napak suite of diopside, there is little evidence for crystallization at high pressure (20 to 25 kbar). Any high-pressure clinopyroxene phenocrysts probably settled out of the ascending melt, or conditions for their crystallization were never satisfied.

It is unlikely that low-pressure differentiation of a *single* parental nephelinitic magma produced a bimodal assemblage of clinopyroxene phenocrysts that not only show reverse zonation but also are out of isotopic equilibrium. Chemical and textural features similar to those shown by the Napak suite of diopside are documented in clinopyroxene phenocrysts from other continental alkaline centers, and have been attributed to open-system behavior, such as magma mixing (*e.g.*, Dobosi & Fodor 1992). Compositional variations in pyroxene from volcanic rocks at West Eifel (Germany) have been attributed to polybaric crystallization within the lithospheric mantle, combined with mixing with a more primitive mantle-derived melt (Duda & Schmincke 1985). Magma mixing (Brooks & Printzlau 1978) has also been favored to explain phenocrysts of reversely zoned clinopyroxenes found in basanite, monchiquite, and leucitite. The bimodality of the diopside phenocrysts from Napak, the chemical variations shown in Figures 2 and 6, and the textural features exhibited in Figure 1, are consistent with the mixing of at least two distinct nephelinitic magmas. The isotopic disequilibrium shown by the diopside populations at Napak requires that the magmas were kept physically separate during their early crystallization, whether in different magma chambers or in a single density-stratified chamber that was undergoing progressive contamination with continental crust (<10 kbar). The fact that both chromian diopside and titanium-bearing aluminian diopside form a core to the clinopyroxene phenocrysts from Napak indicates that mixing must have occurred after crystallization of both populations of diopside in their respective magmas had begun. The examples of normal and reverse zoning that have been found in individual diopside crystals (Fig. 2) indicate continued crystallization of diopside after the two melts mixed. Magma mixing may have occurred at a lower-crust level, a region favorable to the ponding of mantle-derived melts due to density contrasts (*e.g.*, Duda & Schmincke 1985). Basanitic lavas from southern Slovakia (Dobosi & Fodor 1992) contain a bimodal assemblage of core compositions in diopside phenocrysts surrounded by a mantle of uniform composition, and this observation has been used to suggest a model that involves magma mixing. These features also indicate that diopside crystallization subsequent to magma mixing occurred in a melt of uniform composition that did not change throughout the formation of the pyroxene mantles. In contrast, the large compositional variations observed in the pyroxene mantles from Napak indicate that they did not equilibrate in a common melt prior to eruption.

Scavenging a variety of phenocrysts into a single liquid is provided by models for magma-reservoir dynamics that propose the disruption of established compositional and thermal gradients by turbulent injections ("fountains") of hot, dense, primitive liquid (*e.g.*, Turner & Campbell 1986). Stirring or mixing of magmas could be aided by exsolution of CO_2 and H_2O from fresh influxes of volatile-rich, primitive magma. This mechanism may have been important at Napak because of the predominantly pyroclastic nature of the volcanic suite, the presence of a central carbonatite plug, and the abundance of volatiles (particularly CO_2) in nephelinitic magmas (Brey & Green 1977, Brey 1978, Olafsson & Eggler 1983, Wallace & Green 1988). In the case of physically separated magma chambers, mixing could have occurred during eruptive events that tapped multiple chambers with an ascending batch of primitive magma. The reverse zoning and isotopic disequilibrium between the diopside phenocrysts and their surrounding melt support this conclusion.

CONCLUSIONS

The presence of chemically and isotopically distinct populations of diopside phenocrysts in nephelinite from Napak supports a model involving crystallization from distinct mantle-derived melts, and subsequent mixing at shallow crustal levels. Despite the fact that the Cr, Al, and Mg contents of the chromian diopside are similar to those from mantle lherzolite, their lower contents of SiO_2 and Na, and higher contents of Ti, coupled with textural features, indicate that they are not mantle xenocrysts scavenged from a source peridotite. The distinct chemical trends, complex zoning and textural features shown by both suites of diopside are consistent with a magma-mixing model.

ACKNOWLEDGEMENTS

We thank P. Jones and G. Poirier for technical assistance, and J.W. Card and A.D. Fowler for reviews of an earlier version of the manuscript. Three of the samples used in this study were obtained several years ago from the Geological Survey of Uganda. Comments by R.F. Martin, R.H. Mitchell and an anonymous reviewer greatly improved the quality of the manuscript. This work was partly funded by NSERC grant A8314 to K.B.

REFERENCES

ANDERSON, A.T., JR. (1983): Oscillatory zoning of plagioclase: Nomarski interference contrast microscopy of etched polished sections. *Am. Mineral.* **68**, 125-129.

AOKI, K. & KUSHIRO, I. (1968): Some clinopyroxenes from ultramafic inclusions in Dreiser Weiher, Eifel. *Contrib. Mineral. Petrol.* **18**, 326-337.

_____ & SHIBA, I. (1973): Pyroxenes from lherzolite inclusions of Itinomegata, Japan. *Lithos* **6**, 41-51.

BARTON, M. & VAN BERGEN, M.J. (1981): Green clinopyroxenes and associated phases in a potassium-rich lava from the Leucite Hills, Wyoming. *Contrib. Mineral. Petrol.* **77**, 101-114.

BREY, G.P. (1978): Origin of olivine melilitites – chemical and experimental constraints. *J. Volcanol. Geotherm. Res.* **3**, 61-88.

_____ & GREEN, D.H. (1977): Systematic study of liquidus phase relations in olivine melilitite + H_2O + CO_2 at high pressures and the petrogenesis of an olivine melilitite magma. *Contrib. Mineral. Petrol.* **61**, 141-162.

BROOKS, C.K. & PRINTZLAU, I. (1978): Magma mixing in mafic alkaline volcanic rocks: the evidence from relict phenocryst phases and other inclusions. *J. Volcanol. Geotherm. Res.* **4**, 315-331.

BULTITUDE, R.J. & GREEN, D.H. (1971): Experimental study of crystal–liquid relationships at high pressures in olivine nephelinite and basanite compositions. *J. Petrol.* **12**, 121-147.

CLARK, A.H., PEARCE, T.H., ROEDER, P.L. & WOLFSON, I. (1986): Oscillatory zoning and other microstructures in magmatic olivine and augite: Nomarski interference contrast observations on etched polished surfaces. *Am. Mineral.* **71**, 734-741.

COHEN, R.S., O'NIONS, R.K. & DAWSON, J.B. (1984): Isotope geochemistry of xenoliths from East Africa: implications for development of mantle reservoirs and their interaction. *Earth Planet. Sci. Lett.* **68**, 209-220.

DAWSON, J.B. (1987): Metasomatized harzburgites in kimberlite and alkaline magmas: enriched restites and "flushed" lherzolites. *In* Mantle Metasomatism (M.A. Menzies & C.J. Hawkesworth, eds.). Academic Press, London, U.K. (125-144).

DEER, W.A., HOWIE, R.A. & ZUSSMAN, J. (1992): *An Introduction to the Rock-Forming Minerals* (second ed.) Longman Scientific & Technical, Essex, U.K.

DOBOSI, G. & FODOR, R.V. (1992): Magma fractionation, replenishment, and mixing as inferred from green-core clinopyroxenes in Pliocene basanite, southern Slovakia. *Lithos* **28**, 133-150.

DONALDSON, C.H., DAWSON, J.B., KANARIS-SOTIRIOU, R., BATCHELOR, R.A. & WALSH, J.N. (1987): The silicate lavas of Oldoinyo Lengai, Tanzania. *Neues Jahrbuch Mineral., Abh.* **156**, 247-279.

DROOP, G.T.R. (1987): A general equation for estimating Fe^{3+} concentrations in ferromagnesian silicates and oxides from microprobe analyses, using stoichiometric criteria. *Mineral. Mag.* **51**, 431-435.

DUDA, A. & SCHMINCKE, H.-U. (1985): Polybaric differentiation of alkali basaltic magmas: evidence from green-core clinopyroxenes (Eifel, FRG). *Contrib. Mineral. Petrol.* **91**, 340-353.

EGGLER, D.H. (1989): Carbonatites, primary melts, and mantle dynamics. *In* Carbonatites: Genesis and Evolution (K. Bell, ed.). Unwin Hyman, London, U.K. (561-579).

FREESTONE, I.C. & HAMILTON, D.L. (1980): The role of liquid immiscibility in the genesis of carbonatites: an experimental study. *Contrib. Mineral. Petrol.* **73**, 105-117.

KING, B.C. (1949): The Napak area of southern Karamoja, Uganda. *Mem. Geol. Surv. Uganda* **5**, 1-57.

KJARSGAARD, B.A. & HAMILTON, D.L. (1988): Liquid immiscibility and the origin of alkali-poor carbonatites. *Mineral. Mag.* **52**, 43-55.

_____ & _____ (1989a): Carbonatite origin and diversity. *Nature* **338**, 547-548.

_____ & _____ (1989b): Melting experiments on Shombole nephelinites: silicate/carbonate immiscibility, phase relations and the liquid line of descent. *Geol. Assoc. Can. – Mineral. Assoc. Can., Program Abstr.* **14**, A50.

_____ & _____ (1989c): The genesis of carbonatites by immiscibility. *In* Carbonatites: Genesis and Evolution (K. Bell, ed.). Unwin Hyman, London, U.K. (388-404).

_____ & PETERSON, T.D. (1991): Nephelinite–carbonatite liquid immiscibility at Shombole volcano, East Africa: petrographic and experimental evidence. *Mineral. Petrol.* **43**, 293-314.

KOSTER VAN GROOS, A.F. & WYLLIE, P.J. (1966): Liquid immiscibility in the system $Na_2O - Al_2O_3 - SiO_2 - CO_2$ at pressures up to 1 kilobar. *Am. J. Sci.* **264**, 234-255.

_____ & _____ (1968): Liquid immiscibility in the join $NaAlSi_3O_8 - Na_2CO_3 - H_2O$ and its bearing on the genesis of carbonatites. *Am. J. Sci.* **266**, 932-967.

_____ & _____ (1973): Liquid immiscibility in the join $NaAlSi_3O_8 - CaAl_2Si_2O_8 - Na_2CO_3 - H_2O$. *Am. J. Sci.* **273**, 465-487.

KRAMM, U. (1994): Isotope evidence for ijolite formation by fenitization: Sr–Nd data of ijolites from the type locality Iivaara, Finland. *Contrib. Mineral. Petrol.* **115**, 279-286.

LE BAS, M.J. (1987): Nephelinites and carbonatites. *In* Alkaline Igneous Rocks (J.G. Fitton & B.G.J. Upton, eds.). Blackwell, London, U.K. (53-83).

_____ (1989): Diversification of carbonatite. *In* Carbonatites: Genesis and Evolution (K. Bell, ed.). Unwin Hyman, London, U.K. (428-447).

MEYER, H.O.A. & MITCHELL, R.H. (1988): Sapphire-bearing ultramafic lamprophyre from Yogo, Montana: a ouachitite. *Can. Mineral.* **26**, 81-88.

MITCHELL, R.H. (1980): Pyroxenes of the Fen alkaline complex, Norway. *Am. Mineral.* **65**, 45-54.

OLAFSSON, M. & EGGLER, D.H. (1983): Phase relations of amphibole, amphibole-carbonate, and phlogopite-carbonate peridotite: petrologic constraints on the asthenosphere. *Earth Planet. Sci. Lett.* **64**, 305-315.

PEARCE, T.H. & KOLISNIK, A.M. (1990): Observation of plagioclase zoning using interference imaging. *Earth-Sci. Rev.* **29**, 9-26.

PETERSON, T.D. (1989a): Peralkaline nephelinites. I. Comparative petrology of Shombole and Oldoinyo L'engai, East Africa. *Contrib. Mineral. Petrol.* **101**, 458-478.

_____ (1989b): Peralkaline nephelinites II. Low pressure fractionation and the hypersodic lavas of Oldoinyo L'engai. *Contrib. Mineral. Petrol.* **102**, 336-346.

PLATT, R.G. & EDGAR, A.D. (1972): The system nepheline – diopside – sanidine and its significance to the genesis of melilite- and olivine-bearing alkaline rocks. *J. Geol.* **80**, 224-236.

PRINGLE, G.J. (1989): EDDI: A FORTRAN computer program to produce corrected microprobe analyses of minerals using an energy dispersive X-ray spectrometer. *Geol. Surv. Can., Open-File Rep.* **2127**.

REEDER, R.J., FAGIOLI, R.O. & MEYERS, W.J. (1990): Oscillatory zoning of Mn in solution-grown calcite crystals. *Earth-Sci. Rev.* **29**, 39-46.

ROEDER, P.L. & EMSLIE, R.F. (1970): Olivine–liquid equilibrium. *Contrib. Mineral. Petrol.* **29**, 275-289.

SANTACROCE, R., BERTAGNINI, A., CIVETTA, L., LANDI, P. & SBRANA, A. (1993): Eruptive dynamics and petrogenetic processes in a very shallow magma reservoir: the 1906 eruption of Vesuvius. *J. Petrol.* **34**, 383-425.

SCHAIRER, J.F. & YODER, H.S., JR. (1960): The nature of residual liquids from crystallization, with data on the system nepheline – diopside – silica. *Am. J. Sci.* **258A**, 273-283.

SCHULZE, D.J. (1987): Megacrysts from alkalic volcanic rocks. *In* Mantle Xenoliths (P.H. Nixon, ed.). John Wiley & Sons, Chichester, U.K. (433-451).

SHIMIZU, N. (1990): The oscillatory trace element zoning of augite phenocrysts. *Earth-Sci. Rev.* **29**, 27-37.

SIMONETTI, A. & BELL, K. (1993): Isotopic disequilibrium in clinopyroxenes from nephelinitic lavas, Napak volcano, eastern Uganda. *Geology* **21**, 243-246.

_____ & _____ (1994): Nd, Pb and Sr isotopic data from the Napak carbonatite – nephelinite centre, eastern Uganda: an example of open-system crystal fractionation. *Contrib. Mineral. Petrol.* **115**, 356-366.

THOMPSON, R.N. (1973): Oscillatory and sector zoning in augite from a Vesuvian lava. *Carnegie Inst. Wash. Yearbook* **72**, 463-470.

_____ (1974): Some high-pressure pyroxenes. *Mineral. Mag.* **39**, 768-787.

TURNER, J.S. & CAMPBELL, I.H. (1986): Convection and mixing in magma chambers. *Earth-Sci. Rev.* **23**, 255-352.

UPTON, B.G.J., MITCHELL, R.H., LONG, A. & ASPEN, P. (1992): Primitive olivine melanephelinite dykes from the Orkney Islands, Scotland. *Geol. Mag.* **129**, 319-324.

WALLACE, M.E. & GREEN, D.H. (1988): An experimental determination of primary carbonatite magma composition. *Nature* **335**, 343-346.

WASS, S.Y. (1979): Multiple origins of clinopyroxene in alkalic basaltic rocks. *Lithos* **12**, 115-132.

WENDLANDT, R.F. & HARRISON, W.J. (1979): Rare earth partitioning between immiscible carbonate and silicate liquids and CO_2 vapour: results and implications for the formations of light rare earth-enriched rocks. *Contrib. Mineral. Petrol.* **69**, 409-419.

Received October 8, 1994, revised manuscript accepted December 12, 1994.